

Look Before You Leap: Bridging Model-Free and Model-Based Reinforcement Learning for Planned-Ahead Vision-and-Language Navigation

Xin Wang*, Wenhan Xiong*, Hongmin Wang, William Yang Wang

University of California, Santa Barbara
{[xwang](#),[xwhan](#),[hongmin.wang](#),[william](#)}@cs.ucsb.edu

Abstract. Existing research studies on vision and language grounding for robot navigation focus on improving model-free deep reinforcement learning (DRL) models in synthetic environments. However, model-free DRL models do not consider the dynamics in the real-world environments, and they often fail to generalize to new scenes. In this paper, we take a radical approach to bridge the gap between synthetic studies and real-world practices—We propose a novel, planned-ahead hybrid reinforcement learning model that combines model-free and model-based reinforcement learning to solve a real-world vision-language navigation task. Our look-ahead module tightly integrates a look-ahead policy model with an environment model that predicts the next state and the reward. Experimental results suggest that our proposed method significantly outperforms the baselines and achieves the best on the real-world Room-to-Room dataset. Moreover, our scalable method is more generalizable when transferring to unseen environments, and the relative success rate is increased by 15.5% on the unseen test set.

Keywords: Vision-and-Language Navigation, First-Person View Video, Model-based Reinforcement Learning

1 Introduction

It is rather trivial for a human to follow the instruction “*Walk beside the outside doors and behind the chairs across the room. Turn right and walk up the stairs...*”, but teaching robots to navigate with such instructions is a very challenging task. The complexities arise from not just the linguistic variations of instructions, but also the noisy visual signals from the real-world environments that have rich dynamics. Robot navigation via visual and language grounding is also a fundamental goal in computer vision and artificial intelligence, and it is beneficial for many practical applications as well, such as in-home robots, hazard removal, and personal assistants.

* Equal contribution



Walk beside the outside doors and behind the chairs across the room.
 Turn right and walk up the stairs. Stop on the seventh step.

Fig. 1: An example of our task. The embodied agent learns to navigate through the room and arrive at the destination (**green**) by following the natural language instructions. **Red** and **blue** arrows match the orientations depicted in the pictures to the corresponding sentence.

Vision-and-Language Navigation (VLN) is the task of training an embodied agent which has the first-person view as humans to carry out natural language instructions in the real world [1]. Figure 1 demonstrates an example of the VLN task, where the agent moves towards to the destination by analyzing the visual scene and following the natural language instructions. This is different from some other vision & language tasks where the visual perception and natural language input are usually fixed (*e.g.* Visual Question Answering). For VLN, the agent can interact with the real-world environment, and the pixels it perceives are changing as it moves. Thus, the agent must learn to map its visual input to the correct action based on its perception of the world and its understanding of the natural language instruction.

Although steady progress has been made on natural language command of robots [2,3,4,5], it is still far from perfect. Previous methods are mainly employing *model-free* reinforcement learning (RL) to train the intelligent agent by directly mapping raw observations into actions or state-action values. But model-free RL does not consider the environment dynamics and usually requires a large amount of training data. Besides, most of them are evaluated only in synthetic rather than real-world environments, which significantly simplifies the noisy visual & linguistic perception problem, and the subsequent reasoning process in the real world.

It is worth noticing that when humans follow the instructions, however, they do not solely rely on the current visual perception, but also imagine what the environment would look like and plan ahead in mind before actually performing a series of actions. For example, in baseball, the catcher and the outfield players often predict the direction and the rate of speed that the ball will travel, so they can plan ahead and move to the expected destination of the ball. Inspired by this

fact, we seek the help of recent advance of *model-based* RL [6,7] for this task. Model-based RL attempts to learn a model that can be used to simulate the environment and do multi-step lookaheads for planning. With an internal environment model to predict the future and plan ahead, the agent can benefit from the planning while avoiding from some trial-and-error in the real environment.

Therefore, in this paper, we propose a novel approach which improves the vision-and-language navigation task performance by Reinforced Planning Ahead (which we refer as RPA). More specifically, our method, for the first time, endows the intelligent VLN agent with an environment model to simulate the world and predict the future visual perception. Thus the agent can realize directly mapping from the current real observation and planning of the future observations at the same time, and then perform an action based on both. Furthermore, We choose the real-world Room-to-Room (R2R) dataset as the testbed of our method. Our model-free RL model significantly outperforms the baseline methods as reported in the R2R dataset. Moreover, being equipped with the look-ahead module, our RPA model further improves the results and achieves the best on the R2R dataset. Hence, our contributions are three-fold:

- We are the first to combine model-free and model-based DRL for vision-and-language navigation.
- Our proposed RPA model significantly outperforms the baselines and achieves the best on the real-world R2R dataset.
- Our method is more scalable, and its strong generalizability allows it to be better transferred to unseen environments than the model-free RL methods.

2 Method

2.1 Task Definition

As shown in Figure 1, we consider an embodied agent that learns to follow natural language instructions and navigate in realistic indoor environments. Specifically, given the agent’s initial pose $p_0 = (v_0, \phi_0, \theta_0)$, which includes the spatial position, heading and elevation angles, and a natural language instruction (sequence of words) $\mathcal{X} = \{x_1, x_2, \dots, x_n\}$, the agent is expected to choose a sequence of actions $\{a_1, a_2, \dots, a_T\} \in \mathcal{A}$ and arrive at the target position v_{target} specified by the language instruction \mathcal{X} . The action set \mathcal{A} consists of six unique actions, *i.e.* *turn left*, *turn right*, *camera up*, *camera down*, *move forward*, and *stop*. In order to figure out the desired action a_t at each time step, the agent needs to effectively associate the language semantics with its visual observation o_t about the environment. Here the observation o_t is the raw RGB image captured by the mounted camera. The performance of the agent is evaluated by both the success rate P_{succ} (the percentage of test instructions that are correctly followed by the agent) and the final navigation error E_{nav} (average final distance from the target position).

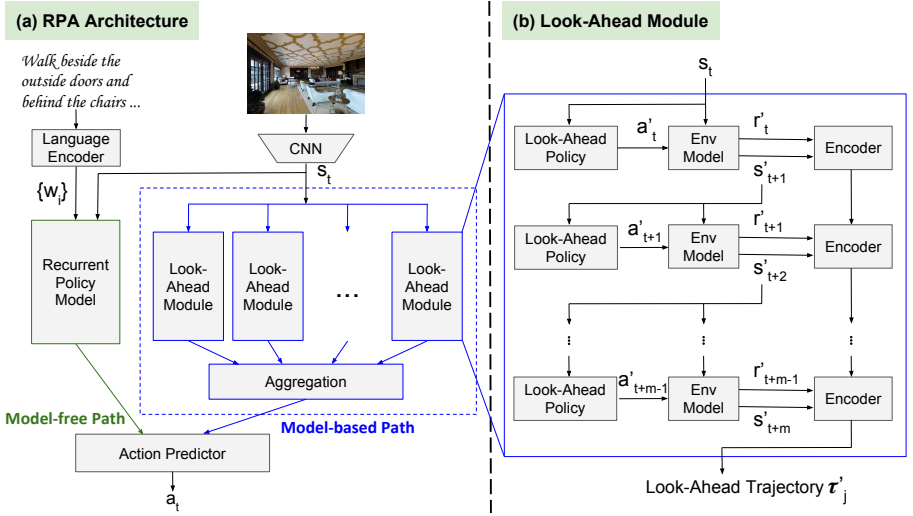


Fig. 2: The overview of our method.

2.2 Overview

In consideration of the sequential-decision making nature of the VLN task, we formulate VLN as a reinforcement learning problem, where the agent sequentially interacts with the environments and learns by trial and error. Once an action is taken, the agent receives a scalar reward $r(a_t, s_t)$ from the environment. The agent’s action a_t at each step is determined by a parametrized policy function $\pi(o_t; \theta)$. The training objective is to find the optimal parameters θ that maximize the discounted cumulative rewards:

$$\max_{\theta} \mathcal{J}^{\pi} = \mathbb{E} \left[\sum_{t=1}^T \gamma^{t-1} r(a_t, s_t) | \pi(o_t; \theta) \right] \quad , \quad (1)$$

where $\gamma \in (0, 1)$ is the discounted factor that reflects the significance of future rewards.

We model the policy function as a sequence-to-sequence neural network that encodes both the language sequence $\mathcal{X} = \{x_1, x_2, \dots, x_n\}$ and image frames $\mathcal{O} = \{o_1, o_2, \dots, o_T\}$ and decodes the action sequence $\{a_1, a_2, \dots, a_T\}$. The basic model consists of a **language encoder** that encodes the instruction \mathcal{X} as word features $\{w_1, w_2, \dots, w_n\}$, an **image encoder** that extracts high-level visual features, and a **recurrent policy network** that decodes actions and recurrently updates its internal state, which is supposed to encode the history of previous actions and observations. To reinforce the agent by planning ahead and further improve the model’s capability, we equip the agent with **look-ahead modules**, which employ the **environment model** to take into account the future predictions.

As illustrated in Figure 2(a), at each time step t , the recurrent policy model takes as input the word features $\{w_i\}$ and the state s_i and produces the infor-

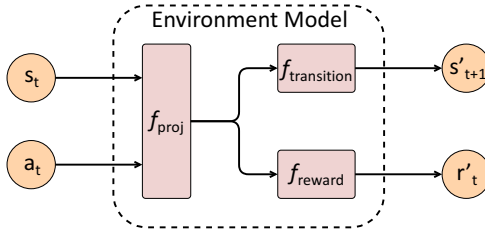


Fig. 3: The environment model.

mation for the final decision making, which forms a *model-free path* by itself. In addition, the *model-based path* exploits multiple look-ahead modules to realize look-ahead planning and imagine the possible future trajectories. The final action a_t is chosen by the **action predictor**, based on the information from both the model-free and model-based paths. Therefore, our RPA method seamlessly integrates model-free and model-based reinforcement learning.

2.3 Look-Ahead Module

The core component of the RPA method is the look-ahead module, which is used to imagine the consequences of planning ahead multiple steps from the current state s_t . In order to augment the agent with imagination, we introduce the *environment model* that makes a prediction about the future based on the state of the present. Since directly predicting the raw RGB image o_{t+1} is very challenging, our environment model, instead, attempts to predict the abstract-state representation s_{t+1} that represents the high-level visual feature.

Figure 2(b) showcases the internal process of the look-ahead module, which consists of an environment model, a look-ahead policy, and a trajectory encoder. Given the abstract-state representation s_t of the real world at step t , the look-ahead policy¹ first takes s_t as input and outputs an imagined action a'_t . Our environment model receives the state s_t and the action a'_t , and predicts the corresponding reward r'_t and the next state s'_{t+1} . Then the look-ahead policy will take a further action a'_{t+1} based on the predicted state s'_{t+1} . The environment model will make a new prediction $\{r'_{t+1}, s'_{t+2}\}$. This look-ahead planning goes m steps, where m is the preset trajectory length. We use an LSTM to encode all the predicted rewards and states along the look-ahead trajectory and outputs its representation τ'_j . As shown in Figure 2(a), at every time step t , our model-based path operates J look-ahead processes and we obtain a look-ahead trajectory representation τ'_j for each ($j = 1, \dots, J$). These J look-ahead trajectories are then aggregated (by concatenation) together and passed to the action predictor as the information of the model-based path.

¹ We adopt the recurrent policy used in the model-free path as the look-ahead policy in all our experiments.

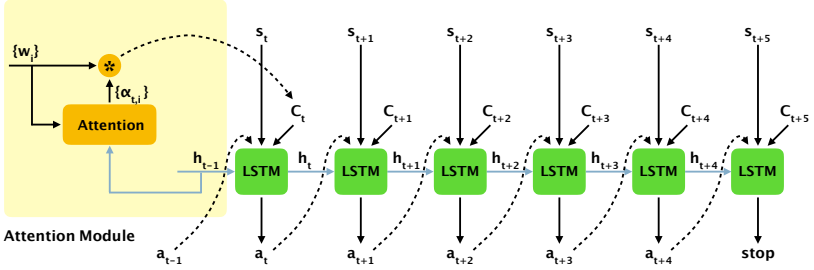


Fig. 4: An example of the unrolled recurrent policy model (from t to $t + 5$). The left-side yellow region demonstrates the attention mechanism at time step t .

2.4 Models

Here we further discuss the architecture designs of the learnable models in our methods that are not specified above, including the environment model, the recurrent policy model, and the action predictor.

Environment Model Given current state s_t and the action a_t taken by the agent, the environment model predicts the next state s'_{t+1} and the reward r'_t . As is shown in Figure 3, the projection function f_{proj} first concatenates s_t and a_t and then projects them into the same feature space. Its output is then fed into the transition function $f_{transition}$ and the reward function f_{reward} to obtain s'_{t+1} and r'_t respectively. In formula,

$$s'_{t+1} = f_{transition}(f_{proj}(s_t, a_t)) \quad (2)$$

$$r'_t = f_{reward}(f_{proj}(s_t, a_t)) \quad , \quad (3)$$

where f_{proj} , $f_{transition}$, and f_{reward} are all learnable neural networks. Specifically, f_{proj} is a linear projection layer, $f_{transition}$ is a multilayer perceptron with sigmoid output, and f_{reward} is also a multilayer perceptron but directly outputs the scalar reward.

Recurrent Policy Model Our recurrent policy model is an attention-based LSTM decoder network (see Figure 4). At each time step t , the LSTM decoder produces the action a_t by considering the context of the word features $\{w_i\}$, the environment state s_t , the previous action a_{t-1} , and its internal hidden state h_{t-1} . Note that one may directly take the encoded word features $\{w_i\}$ as the input of the LSTM decoder. We instead adopt an attention mechanism to better capture the dynamics in the language instruction and dynamically put more attention to the words that are beneficial for the current action selection.

The left-hand side of Figure 4 is a demo attention module for the LSTM decoder. At each time step t , the context vector c_t is computed as a weighted

sum over the encoded word features $\{w_i\}$

$$c_t = \sum \alpha_{t,i} w_i \quad . \quad (4)$$

These attention weights $\{\alpha_{t,i}\}$ act as an alignment mechanism by giving higher weights to certain words which match the decoder’s current status, and are defined as

$$\alpha_{t,i} = \frac{\exp(e_{t,i})}{\sum_{k=1}^n \exp(e_{t,k})} \quad , \quad \text{where } e_{t,i} = h_{t-1}^\top w_i \quad . \quad (5)$$

h_{t-1} is the decoder’s hidden state at previous step.

Once the context vector c_t is obtained, the concatenation of $[c_t, s_t, a_{t-1}]$ is fed as the input of the decoder to produce the intermediate model-free feature for the action predictor’s use. Formally,

$$h_t = LSTM(h_{t-1}, [c_t, s_t, a_{t-1}]) \quad . \quad (6)$$

Then the output feature is the concatenation of the LSTM’s output h_t and the context vector c_t , which will be passed to the action predictor for making the decision. But if the recurrent policy model is employed as an individual policy (*e.g.* the look-ahead policy), then it directly outputs the action a_t based on $[h_t; c_t]$. Note that in our model, we feed the context vector c_t to both the LSTM and the output posterior, which boosts the performance than solely feeding it into the input.

Action Predictor The action predictor is a multilayer perceptron with a Soft-Max layer as the last layer. Given the information from both the model-free and model-based paths as the input, the action predictor generates a probability distribution over the action space \mathcal{A} .

2.5 Learning

The training of the whole system is a two-step process: learning the environment model first and then learning the enhanced policy model, which is equipped with the look-ahead module.

Environment Model Learning Ideally, the look-ahead module is expected to provide the agent with accurate predictions of future observations and rewards. If the environment model is noisy itself, it can actually provide misleading information and make the training even more unstable. In terms of this, before we plug in the look-ahead module, we pretrain the environment model using a randomized teacher policy. Under this policy, the agent will decide whether to take the human demonstration action or a random action based on a Bernoulli meta-policy with $p_{human} = 0.95$. Since the agent’s policy will get closer to demonstration (optimal) policy during training, the environment model trained by demonstration policy will help it better predict the transitions close to the optimal trajectories.

On the other hand, in reinforcement learning methods, the agent’s policy is usually stochastic during training. Making the agent take the random action under the probability of $1 - p_{human}$ is to simulate the stochastic training process. We define two losses to optimize this environment model:

$$l_{transition} = \mathbb{E}[(s'_{t+1} - s_{t+1})^2] \quad (7)$$

$$l_{reward} = \mathbb{E}[(r'_{t+1} - r_{t+1})^2] \quad . \quad (8)$$

The parameters are updated by jointly minimizing these two losses.

Policy Learning With the pretrained environment model, we can incorporate the look-ahead module into the policy model. We first discuss the general pipeline of training the RL agent and then describe how to train the proposed RPA model.

In the VLN task, two distinct supervisions can be used to train the policy model. First, we can use the demonstration actions provided by the simulator to do pure supervised learning. The training objective in this case is to simply maximize the log-likelihood of the demonstration action:

$$\mathcal{J}_{sl} = \mathbb{E}[\log(\pi(a_h|o; \theta))] \quad , \quad (9)$$

where a_h is the demonstration action. This agent can quickly learn a policy that perform relative well on seen scenes. However, pure supervised learning only encourage the agent to imitate the demonstration paths. This potentially limits the agent’s ability to recover from erroneous actions in an unseen environment. To also encourage the agent to explore the state-action space outside the demonstration path, we utilize the second supervision, *i.e.* the reward function. The reward function depends on the environment state s and agent’s action a , and is usually not differentiable in terms of θ . As the objective of the VLN task is to successfully arrive at the target position, we define our reward function based on the distance metric. We denote the distance between a state s and the target position v_{target} as $\mathcal{D}_{target}(s)$. Then the reward after taking action a_t at state s_t is defined as:

$$r(s_t, a_t) = \mathcal{D}_{target}(s_t) - \mathcal{D}_{target}(s_{t+1}) \quad . \quad (10)$$

It indicates whether the action reduces the agents distance from the target. Obviously, this reward function only reflects the immediate effect of a particular action but ignores the action’s future influence. To account for this, we reformulate the reward function in a discounted cumulative form:

$$R(s_t, a_t) = \sum_{t'=t}^T \gamma^{t'-t} r(s_{t'}, a_{t'}) \quad . \quad (11)$$

Besides, the success of the whole trajectory can also be used as an additional binary reward. Further details on reward setting are discussed in the experiment section. With the reward function, the RL objective then becomes:

$$\mathcal{J}_{rl} = \mathbb{E}_{a \sim \pi(\theta)} \left[\sum_t R(s_t, a_t) \right] \quad . \quad (12)$$

Algorithm 1 RL training with planning ahead

```

1:  $\theta_p$ : policy parameters to be learned,  $\theta_e$ : environment model parameters
2: Initialize the R2R environment
3: while not converged do
4:   Roll-out a trajectory ( $\langle s_1, a_1, r_1 \rangle, \langle s_2, a_2, r_3 \rangle, \dots, \langle s_T, a_t, r_T \rangle$ )
5:   Update  $\theta_e$  using  $g \propto \nabla_{\theta_e} (l_{transition} + l_{reward})$ 
6: end while
7: for iteration=0,M-1 do
8:   initialize the weight for supervised loss  $w_{SLoss} \leftarrow 1$ 
9:   Sample a batch of training instructions
10:   $s_0 \leftarrow$  initial state
11:  for  $t = 0, \text{MAX\_EPISODE\_LEN}-1$  do
12:    Perform depth-bounded ( $depth = 2$ ) roll-outs using the environment model
13:    Use roll-out encoder to encoder all these simulated
14:    Sample actions under the current policy in parallel
15:    Save immediate rewards  $r(s_t, a_t)$  and performed actions  $a_t$ 
16:    if All Ended then
17:      Break
18:    end if
19:  end for
20:  Compute the discounted cumulative reward  $R(s_t, a_t)$ 
21:  Total loss  $l_{policy} = -w_{SLoss} * \mathcal{J}_{sl} - (1 - w_{SLoss}) * \mathcal{J}_{rl}$ 
22:  Decrease  $w_{SLoss}$ :  $w_{SLoss} \leftarrow 0.1 + 0.9 * \exp(iteration/T)$ 
23:  Update  $\theta_p$  using  $g \propto \nabla l_{policy}$ 
24: end for

```

Using the likelihood-ratio estimator in the REINFORCE algorithm, the gradient of \mathcal{J}_{rl} can be written as:

$$\nabla_{\theta} \mathcal{J}_{rl} = \mathbb{E}_{a \sim \pi(\theta)} [\nabla_{\theta} \log \pi(a|s; \theta) R(s, a)] \quad . \quad (13)$$

With this two training objective, we can either use a mixed loss function as in [8] to train the whole model, or use the supervised learning to warm-start the model and use RL to do fine-tuning. In our case, we find the mixed loss converges faster and achieves better performance.

To joint train the policy model and look-ahead module, we first freeze the pretrained environment model. Then at each step, we perform simulated depth-bounded roll-outs using the environment model. Since we have five unique actions besides the *stop* action, we perform the corresponding five roll-outs. Each path is first encoded using an LSTM. The last hidden states of all paths are concatenated and then feed into action predictor. Now the learnable parameters come from three components: the original model-free policy mode, the roll-out encoder, and the action predictor. The pseudo-code of the algorithm is shown in Algorithm 1.

3 Experiments

3.1 Experimental Settings

R2R Dataset Room-to-Room (R2R) dataset [1] is the first dataset for vision-and-language navigation task in real 3D environments. The R2R dataset is built upon the Matterport3D dataset [9], which consists of 10,800 panoramic views constructed from 194,400 RGB-D images of 90 building-scale scenes (Many of the scenes can be viewed in the Matterport 3D spaces gallery²). The R2R dataset further samples 7,189 paths capturing most of the visual diversity in the dataset and collects 21,567 navigation instructions with an average length of 29 words (each path is paired with 3 different instructions). As reported in [1], the R2R dataset is split into training (14,025 instructions), seen validation (1,020), unseen validation (2,349), and test (4,173) sets. Both the unseen validation and test sets contain environments that are unseen in the training set, while the seen validation set shares the same environments with the training set. Because the test set will not be released as they claimed, we hold the seen validation and unseen validation as our two test sets (*test seen* and *test unseen*), and separately use 1/10 of the training set as our validation set in all our experiments.

Implementation Details We develop our algorithms on the open source code of the Matterport3D simulator³. ResNet-152 CNN features [10] are extracted for all the images without fine-tuning. In the model-based path, we perform one look-ahead planning for each possible action in the environment. The j -th look-ahead planning corresponds to the j -th of the action set \mathcal{A} , and the subsequent actions are executed by the shared look-ahead policy. In our experiments, we use the same policy model trained in the model-free path as the look-ahead policy. All the other hyperparameters are tuned on the validation set. More training details can be found in the supplementary material.

Evaluation Metrics Following the conventional wisdom, the R2R dataset mainly evaluates the results by three metrics: navigation error, success rate, and oracle success rate. The navigation error is defined as the shortest path distance in the navigation graph between the agent’s final position v_T and the destination v_{target} . The success rate calculates the percentage of the result trajectories whose navigation errors are less than 3m. The oracle success rate is also reported: the distance between the closest point on the trajectory and the destination is used to calculate the error, even if the agent does not stop there.

Baselines In the R2R dataset, there exists a ground-truth shortest-path trajectory (*Shortest*) for each instruction sequence from the starting location v_0 to the target location v_{target} . This shortest-path trajectory can be further used

² <https://matterport.com/gallery/>

³ <https://github.com/peteanderson80/Matterport3DSimulator>

Table 1: Results on both the Test Seen and Test Unseen sets. We list the best results as reported in [1], of which Student-forcing performs the best. Our RPA method significantly outperforms the previous best results, and it is also noticeable that we gain a larger improvement on Test Unseen than Test Seen, which proves that our RPA method is more generalized.

Model	Test Seen			Test Unseen		
	Navigation Error (m)	Success (%)	Oracle Success (%)	Navigation Error (m)	Success (%)	Oracle Success (%)
Shortest	0.00	100.0	100.0	0.00	100.0	100.0
Random	9.45	15.9	21.4	9.23	16.3	22.0
Teacher-forcing[1]	8.42	25.1	35.7	8.81	18.0	27.4
Student-forcing[1]	6.46	35.1	48.0	8.15	19.5	26.1
Ours						
Att-all	5.79	40.2	54.1	7.97	21.3	28.7
Model-free RL	5.82	41.9	53.5	7.88	21.5	28.9
RPA	5.56	42.9	52.6	7.65	24.6	31.8

for supervised training. *Teacher-forcing* [11] uses cross-entropy loss to train the model at each time step to maximize the likelihood of the next ground-truth action given the previous ground-truth action. Instead of feeding the ground-truth action back to the recurrent model, one can sample an action based on the output probabilities over the action space (*Student-forcing*). In our experiments, we list the results of these two models as reported in [1] as our baselines. We also include the results of a random agent (*Random*), which randomly takes an action at each step.

3.2 Results and Analysis

Table 1 shows the result comparison between our models and the baseline models. We first implement our own recurrent policy model (*Att-all*) whose model capacity is much stronger than the baseline models. Both trained with the cross-entropy loss and sampling, our Att-all model significantly outperforms the previous best model (*Student-forcing*) across all the metrics on both test sets (the absolute success rate is improved by 5.1% on Test Seen and 1.8% on Test Unseen). By switching to the model-free RL, the results are slightly improved. Then our RPA learning method further boosts the performance consistently on the metrics and achieves the best results in the R2R dataset (the overall boost of the success rate is 7.8% on Test Seen and 5.1% on Test Unseen), which validates the effectiveness of combining model-free and model-based RL for the VLN task.

An important fact revealed here is that our RPA method brings a notable improvement on the Test Unseen set and the improvement is even larger than that on the Test Seen set (the relative success rates are improved by 6.7% on Test Seen and 15.5% on Test Unseen over Att-all). While the model-free RL method gains very slight performance boost on the Test Unseen set. This proves our

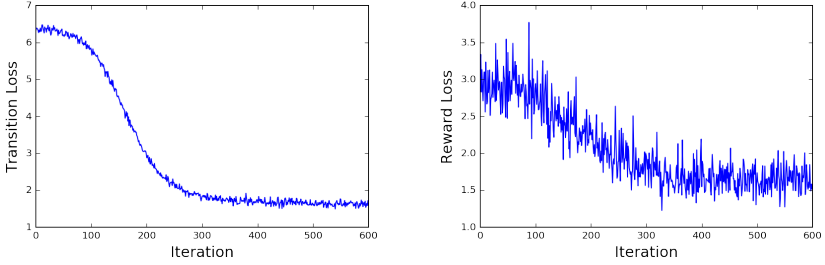


Fig. 5: Learning curves of the environment model.

claim that it is easy to collect and utilize data in a scalable way to incorporate the look-ahead module for the decision making. Besides, our RPA method turns out to be more generalized and can be better transferred to unseen environments.

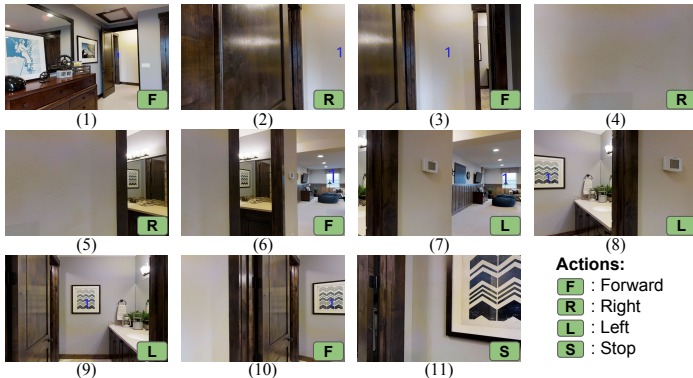
3.3 Ablative Study

Learning Curves of the Environment Model To realize our RPA method, we first need to train an environment model to predict the future state given the present state, which would be then plugged into the look-ahead module. So it is important to guarantee the effectiveness of the pretrained environment model. In Figure 5, we plot both the transition loss and the reward loss of the environment model during training. Evidently, both losses converge to a stable point after around 500 iterations. But it is also noticeable that learning curve of the reward loss is much more noisy than that of the transition loss. This is because of the sparsity nature of rewards. Unlike the state transitions that are usually more continuous, the rewards within trajectory samples are very sparse and of high variance, thus it is more noisy to predict the exact reward using mean square error.

Effect of Different Rewards We test four different reward functions in our experiments. The results are shown in Table 2. The *Global Distance* reward function is defined per path by assigning the same reward to all actions along this path. This reward measures how far the agent approaches the target by finishing the path. The *Success* reward is a binary reward: if the path is correct, then all actions will be assigned with reward 1, otherwise reward 0. The *Discounted* reward is defined as in Equation 11. Finally, the *Discounted & Success* reward, which is used by our final model, basically adds the *Success* binary reward to the immediate reward (see Equation 10) of the final action. Then the discounted cumulative reward is calculated using the Equation 11. In the experiments, the first two rewards are much less effective than the discounted reward functions which assign different rewards to different actions. We believe the discounted reward calculated at every time step can better reflect the true value of each action. As the final evaluation is not only based on the navigation error but also

Table 2: Results of the model-free RL with different reward definitions.

Reward	Test Seen			Test Unseen		
	Navigation Error (m)	Success (%)	Oracle Success (%)	Navigation Error (m)	Success (%)	Oracle Success (%)
<i>Global Distance</i>	6.17	35.5	45.1	8.20	19.0	25.6
<i>Success</i>	6.21	37.8	43.2	8.17	21.3	26.7
<i>Discounted</i>	5.79	40.5	52.8	7.74	20.4	28.5
<i>Discounted & Success</i>	5.82	41.9	53.5	7.88	21.5	28.9



Exit bedroom into hallway. Turn right and then walk into doorway on the left. Stop in the middle of the bathroom next to bathroom sink.

Fig. 6: An example trajectory executed by our RPA agent. Given the instruction and the starting position (1), the agent produces one action per time step. In this example we show all the 11 steps of this trajectory.

success rate, we also observe that incorporating the success information into the reward can further boost the performance in terms of success rate.

Case Study For a more intuitive view of the decision-making process in the VLN task, we show a test trajectory that is performed by our RPA agent in Figure 6. The agent starts from position (1) and takes a sequence of actions by following the natural language instruction until it reaches the destination (11) and stops there. We observe that although the actions include *Forward*, *Left*, *Right*, *Up*, *Down*, and *Stop*, the action *Up* and *Down* appear very rare in the result trajectories. In most cases, the agent can still reach the destination even without moving up/down the camera, which indicates that the R2R dataset has its limitation on the action distribution.

4 Related Work

Vision, Language and Navigation Recently, the intersection of vision and language research has attracted a lot of attention. Much work [12,13,14,15,16,17]

has been done in language generation conditioned on visual inputs. There is also another line of work [18,19] that tries to answer questions from images. The task of vision-language grounding [20,21,22] is more relevant to our task, which requires the ability to connect the language semantics to the physical properties of the environment. Our task requires the same ability but is more task-driven. The agent in our task needs to sequentially interact with the environment and finish a navigation task specified by a language instruction.

Early approaches [23,24,25,26] on robot navigation usually require a prior global map or needs to build an environment map on-the-fly. The navigation goal in these methods is usually directly annotated in the map. In contrast to these work, the VLN task is more challenging in the sense that no global map is required and the goal is not directly annotated but described by natural language. Under this setting, several methods have been proposed recently. Mei *et al.* [27] proposed a sequence-to-sequence model to map the language to navigation actions. Misra *et al.* [5] formulates navigation as a sequential-decision process and proposes to use reward shaping to effectively train the RL agent. However, these methods still operate in synthetic environments and consider either simple discrete observation inputs or unrealistic top-down view of the environment.

Model-based Reinforcement Learning Using model-based RL for planning is a long-standing problem in reinforcement learning. Recently, the great computational power of neural networks makes it more realistic to learn a neural model to simulate environments [28,29,30]. But for more complicated environments where the simulator is not exposed to the agent, the model-based RL usually suffers from the mismatch between the learned and real environments [31,32]. In order to combat this issue, RL researchers are actively working on combining model-free and model-based RL [33,34,35,36]. Most recently, Oh *et al.* [6] propose a Value Prediction Network whose abstract states are trained to make predictions of future values rather than of future observations, and Weber *et al.* [7] introduce an imagination-augmented agent to construct implicit plans and interpret predictions. Our algorithm shares the same spirit and is derived from these methods. But instead of testing on games, we, for the first time, adapt the combination of model-based and model-free RL for the real-world vision-and-language task.

5 Conclusion

Through experiments, we demonstrate the superior performance of our proposed RPA approach, which also tackles the common generalization issue of the model-free RL when applying to unseen scenes. Besides, equipped with the look-ahead module, our method can simulate the environment and incorporate the imagined trajectories, making the model more scalable than the model-free agents. In the future, we plan to explore the potential of the model-based RL to transfer

across different tasks, *i.e.* Vision-and-Language Navigation, Embodied Question Answering [37] etc.

References

1. Anderson, P., Wu, Q., Teney, D., Bruce, J., Johnson, M., Sünderhauf, N., Reid, I., Gould, S., Hengel, A.v.d.: Vision-and-language navigation: Interpreting visually-grounded navigation instructions in real environments. *arXiv preprint arXiv:1711.07280* (2017)
2. Beattie, C., Leibo, J.Z., Teplyashin, D., Ward, T., Wainwright, M., Küttler, H., Lefrancq, A., Green, S., Valdés, V., Sadik, A., et al.: Deepmind lab. *arXiv preprint arXiv:1612.03801* (2016)
3. Kempka, M., Wydmuch, M., Runc, G., Toczek, J., Jaśkowski, W.: Vizdoom: A doom-based ai research platform for visual reinforcement learning. In: *Computational Intelligence and Games (CIG), 2016 IEEE Conference on, IEEE* (2016) 1–8
4. Zhu, Y., Mottaghi, R., Kolve, E., Lim, J.J., Gupta, A., Fei-Fei, L., Farhadi, A.: Target-driven visual navigation in indoor scenes using deep reinforcement learning. In: *Robotics and Automation (ICRA), 2017 IEEE International Conference on, IEEE* (2017) 3357–3364
5. Misra, D.K., Langford, J., Artzi, Y.: Mapping instructions and visual observations to actions with reinforcement learning. *arXiv preprint arXiv:1704.08795* (2017)
6. Oh, J., Singh, S., Lee, H.: Value prediction network. In: *Advances in Neural Information Processing Systems*. (2017) 6120–6130
7. Weber, T., Racanière, S., Reichert, D.P., Buesing, L., Guez, A., Rezende, D.J., Badia, A.P., Vinyals, O., Heess, N., Li, Y., et al.: Imagination-augmented agents for deep reinforcement learning. *arXiv preprint arXiv:1707.06203* (2017)
8. Ranzato, M., Chopra, S., Auli, M., Zaremba, W.: Sequence level training with recurrent neural networks. *arXiv preprint arXiv:1511.06732* (2015)
9. Chang, A., Dai, A., Funkhouser, T., Halber, M., Nießner, M., Savva, M., Song, S., Zeng, A., Zhang, Y.: Matterport3d: Learning from rgb-d data in indoor environments. *arXiv preprint arXiv:1709.06158* (2017)
10. He, K., Zhang, X., Ren, S., Sun, J.: Deep residual learning for image recognition. In: *Proceedings of the IEEE conference on computer vision and pattern recognition*. (2016) 770–778
11. Luong, M.T., Pham, H., Manning, C.D.: Effective approaches to attention-based neural machine translation. *arXiv preprint arXiv:1508.04025* (2015)
12. Xu, K., Ba, J., Kiros, R., Cho, K., Courville, A., Salakhudinov, R., Zemel, R., Bengio, Y.: Show, attend and tell: Neural image caption generation with visual attention. In: *International Conference on Machine Learning*. (2015) 2048–2057
13. Vinyals, O., Toshev, A., Bengio, S., Erhan, D.: Show and tell: A neural image caption generator. In: *Computer Vision and Pattern Recognition (CVPR), 2015 IEEE Conference on, IEEE* (2015) 3156–3164
14. Karpathy, A., Fei-Fei, L.: Deep visual-semantic alignments for generating image descriptions. In: *Proceedings of the IEEE conference on computer vision and pattern recognition*. (2015) 3128–3137
15. Chen, X., Lawrence Zitnick, C.: Mind’s eye: A recurrent visual representation for image caption generation. In: *Proceedings of the IEEE conference on computer vision and pattern recognition*. (2015) 2422–2431

16. Yu, H., Wang, J., Huang, Z., Yang, Y., Xu, W.: Video paragraph captioning using hierarchical recurrent neural networks. In: Proceedings of the IEEE conference on computer vision and pattern recognition. (2016) 4584–4593
17. Wang, X., Chen, W., Wu, J., Wang, Y.F., Wang, W.Y.: Video captioning via hierarchical reinforcement learning. CVPR (2018)
18. Huang, T.H.K., Ferraro, F., Mostafazadeh, N., Misra, I., Agrawal, A., Devlin, J., Girshick, R., He, X., Kohli, P., Batra, D., et al.: Visual storytelling. In: Proceedings of the 2016 Conference of the North American Chapter of the Association for Computational Linguistics: Human Language Technologies. (2016) 1233–1239
19. Antol, S., Agrawal, A., Lu, J., Mitchell, M., Batra, D., Lawrence Zitnick, C., Parikh, D.: Vqa: Visual question answering. In: Proceedings of the IEEE International Conference on Computer Vision. (2015) 2425–2433
20. Thomason, J., Sinapov, J., Mooney, R.: Guiding interaction behaviors for multi-modal grounded language learning. In: Proceedings of the First Workshop on Language Grounding for Robotics. (2017) 20–24
21. Alomari, M., Duckworth, P., Hogg, D.C., Cohn, A.G.: Learning of object properties, spatial relations, and actions for embodied agents from language and vision. In: The AAAI 2017 Spring Symposium on Interactive Multisensory Object Perception for Embodied Agents Technical Report SS-17-05, AAAI Press (2017) 444–448
22. Alomari, M., Duckworth, P., Hawasly, M., Hogg, D.C., Cohn, A.G.: Natural language grounding and grammar induction for robotic manipulation commands. In: Proceedings of the First Workshop on Language Grounding for Robotics. (2017) 35–43
23. Kim, D., Nevatia, R.: Symbolic navigation with a generic map. *Autonomous Robots* **6**(1) (1999) 69–88
24. Borenstein, J., Koren, Y.: Real-time obstacle avoidance for fast mobile robots. *IEEE Transactions on systems, Man, and Cybernetics* **19**(5) (1989) 1179–1187
25. Borenstein, J., Koren, Y.: The vector field histogram-fast obstacle avoidance for mobile robots. *IEEE transactions on robotics and automation* **7**(3) (1991) 278–288
26. Oriolo, G., Vendittelli, M., Ulivi, G.: On-line map building and navigation for autonomous mobile robots. In: Robotics and Automation, 1995. Proceedings., 1995 IEEE International Conference on. Volume 3., IEEE (1995) 2900–2906
27. Mei, H., Bansal, M., Walter, M.R.: Listen, attend, and walk: Neural mapping of navigational instructions to action sequences. In: AAAI. Volume 1. (2016) 2
28. Watter, M., Springenberg, J., Boedecker, J., Riedmiller, M.: Embed to control: A locally linear latent dynamics model for control from raw images. In: Advances in neural information processing systems. (2015) 2746–2754
29. Lenz, I., Knepper, R.A., Saxena, A.: Deepmpc: Learning deep latent features for model predictive control. In: Robotics: Science and Systems. (2015)
30. Finn, C., Levine, S.: Deep visual foresight for planning robot motion. In: Robotics and Automation (ICRA), 2017 IEEE International Conference on, IEEE (2017) 2786–2793
31. Gu, S., Lillicrap, T., Sutskever, I., Levine, S.: Continuous deep q-learning with model-based acceleration. In: International Conference on Machine Learning. (2016) 2829–2838
32. Talvitie, E.: Agnostic system identification for monte carlo planning. In: AAAI. (2015) 2986–2992
33. Sutton, R.S.: Integrated architectures for learning, planning, and reacting based on approximating dynamic programming. In: Machine Learning Proceedings 1990. Elsevier (1990) 216–224

34. Yao, H., Bhatnagar, S., Diao, D., Sutton, R.S., Szepesvári, C.: Multi-step dyna planning for policy evaluation and control. In: *Advances in Neural Information Processing Systems*. (2009) 2187–2195
35. Tamar, A., Wu, Y., Thomas, G., Levine, S., Abbeel, P.: Value iteration networks. In: *Advances in Neural Information Processing Systems*. (2016) 2154–2162
36. Silver, D., van Hasselt, H., Hessel, M., Schaul, T., Guez, A., Harley, T., Dulac-Arnold, G., Reichert, D., Rabinowitz, N., Barreto, A., et al.: The predictron: End-to-end learning and planning. *arXiv preprint arXiv:1612.08810* (2016)
37. Das, A., Datta, S., Gkioxari, G., Lee, S., Parikh, D., Batra, D.: Embodied Question Answering. In: *Proceedings of the IEEE Conference on Computer Vision and Pattern Recognition (CVPR)*. (2018)

A Error Analysis

In addition to the quantitative results on the evaluation metrics, here we further analyze the negative results and demonstrate three kinds of common errors in the vision-and-language navigation task.

First, the existing agents lack the ability to understand the instructions with out-of-vocabulary (OOV) words. During training, the agent can only see the words in the vocabulary and there are no special mechanisms aiming to resolve the OOV issue. Figure 7(a) illustrates such an error case where an OOV word (*pottery*) appears in the instruction, and the agent fails to identify the *pottery* on its right in the scene and mistakenly turns left and then goes forward. Utilizing external knowledge might be a good way to relieve the OOV issue.

Moreover, we show in Figure 7(b) another error case where the agent is required to follow an ambiguous instruction in a relatively complex unseen environment. More specifically, it is asked to “*face the wall with the large painting and four chairs*”, but there are paintings on every wall in the scene, how *large* the painting should be? The instruction actually refers to the larger one shown in the top right corner of the picture (2), but the agent fails to perceive it and thus performs the wrong actions. Therefore it is a must for the agent to have a better understanding of the instruction and the ability to reason about the visual scene to avoid such errors.

The last case we discuss here is the error accumulation issue. Once the agent chooses some wrong actions, it is very likely that the sight of the agent is completely changed. So if the agent cannot fix the errors by itself, the instruction is not “correct” anymore based on the new scene after the wrong actions are taken. Figure 7(c) demonstrates one of the error accumulation cases where one bad decision leads to a series of bad decisions along the navigation process. All these issues mentioned above remain to be solved in future work.

B Network Architecture

In this section, we provide the details of the neural network architectures used for the experiments.

Language Encoder The language encoder is a long short-term memory (LSTM) network with hidden size 512. It takes as input the sequence of word embeddings of the natural language instruction. The word embedding dimension is 256. Then the outputs of the LSTM are passed through a linear layer (512,512) to obtain the final output. Therefore, it follows: Input \rightarrow Embedding (256) \rightarrow LSTM (512) \rightarrow Linear (512, 512) \rightarrow Tanh \rightarrow Output.

Recurrent Policy Model The recurrent policy model consists of an action embedding layer of size 32, a LSTM decoder with hidden size 512, a dot-product attention module, and a projection module (Linear (1024, 512) \rightarrow Tanh \rightarrow Linear

$(512, 6) \rightarrow \text{SoftMax}$) that projects the concatenation of the decoder’s output and the context vector into the probabilities of all actions. Note that if the recurrent policy model works as an individual policy, then it outputs the probabilities of all actions, which is the output of the projection module; while when employed in the model-free path, it directly passes the concatenation of the decoder’s output and the context vector as the representation of the model-free path (the projection module is not used).

Environment Model As shown in Figure 3, the environment model is composed of a projection function (Linear $(256+2048, 512) \rightarrow \text{ReLU}$), transition function (Linear $(512, 256) \rightarrow \text{ReLU} \rightarrow \text{Linear} (256, 512) \rightarrow \text{ReLU} \rightarrow \text{Linear} (512, 2048) \rightarrow \text{Sigmoid}$), and a reward function (Linear $(512, 256) \rightarrow \text{ReLU} \rightarrow \text{Linear} (256, 1)$). Besides, the environment model has its own action embedding layer of size 256.

Trajectory Encoder The trajectory encoder is a LSTM encoder of size 256, which encodes the sequence of the predicted states and rewards (by concatenation). Its output, the encoded vector, is the hidden state of the LSTM at the last step h_t . We concatenate the encoded vectors of all look-ahead planning as the final representation of the model-based path.

Action Predictor The action predictor is a multilayer perceptron: Linear $(256 \times 5 + 1024, 512) \rightarrow \text{ReLU} \rightarrow \text{Linear} (512, 256) \rightarrow \text{ReLU} \rightarrow \text{Linear} (256, 6) \rightarrow \text{SoftMax}$.

C Training Details

We tune all the hyperparameters on the validation set. Here we show the hyperparameter settings of both the RPA agent training and the environment model training.

RPA Agent Hyperparameter Setting We set the maximal length of the action path as 20. The batch size is 100 and the maximum number of iterations is 40,000. We use the Adam optimizer with a learning rate of $1e-4$ to optimize all parameters. To avoid exploding gradients, we clip the gradients of all parameters with a norm of 5. We also use a L2 weight decay of 0.0005 and a dropout ratio of 0.5 to prevent overfitting. The discounted factor of our cumulative reward is 0.95. For the mixed loss, we initialize the weight of the supervised loss as 1.0 and set its lower bound as 0.15. In other words, the weight of supervised loss will never be less than 0.15. We observe that smaller weights of the supervised loss often lead to worse performance on the test samples in seen environments. At every time step, we run 5 individual look-ahead planning, each corresponds to one of the valid actions (except *STOP*). The look-ahead length that achieves the best performance is 2.

Environment Model Hyperparameter Setting The batch size is also set as 100. We use the Adam optimizer with a learning rate of $1e-5$. We also use a L2 weight decay of 0.0005 and a dropout ratio of 0.5 to prevent overfitting. The final loss is a weighted sum of the transition loss and the reward loss, whose weights are 1 and 0.001 correspondingly. We notice that both the transition loss and reward loss converge to a stable point after around 500 iterations.



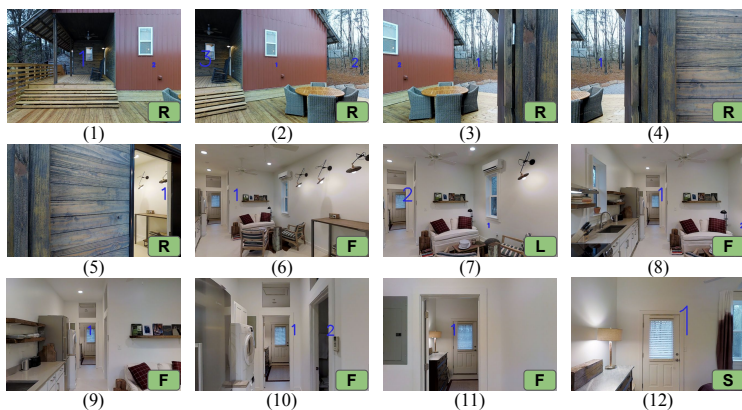
Go to the pottery. Go to the bar. Go to the microwave.

(a) An error case with the OOV word *pottery*.



Face the wall with the large painting and four chairs. Walk to the right of the chairs though the open door. Walk straight through the room and stop in the doorway.

(b) Complex unseen environment and ambiguous instruction.



With the stairs leading down to your left, move forward and climb the four steps to the higher porch. Continue forward and stand in the entrance to the building on your right.

(c) Error accumulation.

Fig. 7: Error cases. Please see Section A for explanation.